Eva Tomas,[1] Violeta Stanojevic,[1] Karen McManus,[1] Ashok Khatri,[1] Paul Everill,[2] William W. Bachovchin,[2] and Joel F. Habener[1]

CrossMark

GLP-1(32-36)amide Pentapeptide Increases Basal Energy Expenditure and Inhibits Weight Gain in Obese Mice

METABOLISM

The prevalence of obesity-related diabetes is increasing worldwide. Here we report the identification of a pentapeptide, GLP-1(32-36)amide (LVKGRamide), derived from the glucoincretin hormone GLP-1, that increases basal energy expenditure and curtails the development of obesity, insulin resistance, diabetes, and hepatic steatosis in diet-induced obese mice. The pentapeptide inhibited weight gain, reduced fat mass without change in energy intake, and increased basal energy expenditure independent of physical activity. Analyses of tissues from peptide-treated mice reveal increased expression of UCP-1 and UCP-3 in brown adipose tissue and increased UCP-3 and inhibition of acetyl-CoA carboxylase in skeletal muscle, findings consistent with increased fatty acid oxidation and thermogenesis. In palmitate-treated C2C12 skeletal myotubes, GLP-1(32-36)amide activated AMPK and inhibited acetyl-CoA carboxylase, suggesting activation of fat metabolism in response to energy depletion. By mass spectroscopy, the pentapeptide is rapidly formed from GLP-1(9-36) amide, the major form of GLP-1 in the circulation of mice. These findings suggest that the reported insulin-like actions of GLP-1 receptor agonists that occur independently of the GLP-1 receptor might be mediated by the pentapeptide, and the previously reported nonapeptide (FIAWLVKGRamide). We propose that by increasing basal energy expenditure, GLP-1(32-36)amide might be a useful treatment for human obesity and associated metabolic disorders.

The prevalence of obesity and associated diabetes and metabolic disorders has increased dramatically over the past 20 years. Obesity-related metabolic disorders are manifested as insulin resistance, diabetes, hypertension, hyperlipidemia, hepatic steatosis, and accelerated atherosclerosis. Although the pathophysiology underlying these disorders remains unknown, insulin resistance appears to be a major contributor (1–4). Currently, effective treatments for obesity are not available. Here we report that a pentapeptide, GLP-1(32-36)amide (LVKGRamide), derived from the C terminus of the glucoincretin hormone GLP-1, increases basal energy expenditure, inhibits weight gain, reduces fat mass, and reduces the development of insulin resistance and hepatic steatosis when administered to diet-induced obese (DIO) mice.

GLP-1 receptor agonists are in use for the treatment of type 2 diabetes based on their stimulation of insulin secretion and a lowering of glucagon levels (5,6). The full-length receptor agonist GLP-1(7-36)amide is rapidly inactivated in the circulation via cleavages by the endopeptidase dipeptidyl peptidase-4 (Dpp4) and a neutral endopeptidase (NEP 24.11) known as neprilysin (7,8). The cleavage of GLP-1(7-36)amide by Dpp4 gives rise to GLP-1(9-36)amide devoid of insulin-releasing activities, and NEP 24.11 cleaves GLP-1 into several small peptides (9). Earlier we proposed that cleavages of GLP-1 by the endopeptidase neprilysin generate a pentapeptide and a nonapeptide, GLP-1(28-36)amide (FIAWLVKGRamide), with insulin-like actions on insulin-responsive target tissues (10). GLP-1(9-36)amide, the product of cleavage of GLP-1 by Dpp4, exerts insulin-like and antioxidant actions on the heart (11–14) and vasculature (15) and suppresses glucose production both in isolated mouse hepatocytes (16) and in obese, insulin-resistant human subjects without effect on plasma insulin levels (17).

[1]Laboratory of Molecular Endocrinology and Department of Medicine, Massachusetts General Hospital, Harvard Medical School, Boston, MA
[2]Department of Biochemistry, Tufts University, Boston, MA

Corresponding author: Joel F. Habener, jhabener@partners.org.

The administration of GLP-1(9-36)amide or the nonapeptide to obese mice increases energy expenditure, curtails weight gain, and inhibits the development of insulin resistance, diabetes, and hepatic steatosis (18,19). In obese mice, the nonapeptide promotes glucose disposal and β-cell regeneration in streptozotocin-induced diabetic mice (20), protects β-cells against glucolipotoxic stress (21), and suppresses hepatic glucose production in obese mice (22). The nonapeptide appears to enter isolated insulin-resistant mouse hepatocytes in vitro, targets to mitochondria, suppresses glucose production and reactive oxygen species, and restores cellular ATP levels that are depleted by oxidative stress (22,23). The actions of the peptides appear to occur preferentially in obese, insulin-resistant compared with lean, insulin-sensitive human subjects (17) or mice (19) and occur by mechanisms independent of the GLP-1 receptor (10,24). Because both peptides are major end products of the proteolysis of GLP-1 by neprilysin (9) in addition to the nonapeptide, we investigated the actions of the pentapeptide (10) in DIO mice. We find that the pentapeptide increases basal energy expenditure, curtails weight gain, and inhibits the development of insulin resistance, diabetes, and hepatic steatosis independently of energy intake or physical activity. The expression of the uncoupling proteins UCP-1 and UCP-3 is increased in the brown adipose tissue (BAT), as is UCP-3 in skeletal muscle of obese mice in response to GLP-1(32-36)amide, findings consistent with an increase in basal energy expenditure. In addition, the activity of acetyl-CoA carboxylase is inhibited in the skeletal muscle of the peptide-treated mice, indicative of an increase in fatty acid oxidation. In C2C12 skeletal myotubes in vitro, GLP-1(32-36)amide activates AMPK and inhibits acetyl-CoA carboxylase (ACC), further supporting increased fatty acid oxidation. These findings of novel energy-modulatory actions of the pentapeptide in obese mice suggest the possibility that it might be an effective treatment for obesity-related diabetes.

RESEARCH DESIGN AND METHODS

Peptide Synthesis
GLP-1(LVKGRamide) was synthesized by solid phase methods. The peptide was purified to a single component on HPLC, and by mass spectroscopy the product molecular weight was 571.38.

Animal Studies
C57BL/6J male mice of 6–9 weeks of age were obtained from The Jackson Laboratory (Bar Harbor, ME). Mice were housed four per cage under a light/dark cycle of 12 h with free access to food and water, except when noted. Mice were fed a regular laboratory chow (10 kcal % fat, D12450B; Research Diets) or a high-fat diet (HFD) (60 kcal % fat, D12492; Research Diets) throughout the studies. All procedures were approved by the Massachusetts General Hospital Institutional Animal Care and Use Committee.

Formation of GLP-1(32-36)amide From GLP-1(9-36) amide in Plasma
Mice 21 weeks of age on a regular laboratory chow or HFD for 15 weeks were given intraperitoneal injections of 500 µg of GLP-1(9-36)amide. Blood samples were collected from the tail vein at 0, 5, and 15 min and by cardiac puncture at 30 min after the administration of GLP-1 (9-36)amide. Plasmas were analyzed for the formation of GLP-1(32-36)amide. Peptide extraction was performed by acetonitrile precipitation (25,26) and detection by liquid chromatography–mass spectroscopy (LC-MS) with an Agilent 1200 HPLC and Applied Biosystems Qtrap 4000 mass spectrometer with a Turbo Spray ion source.

GLP-1(32-36)amide Infusion Studies
At 6–10 weeks of age, mice were placed on an HFD for 7–22 weeks. At 13–28 weeks of age, mice were randomized by average body weight (vehicle group, 38.1 g; peptide treated group, 37.3 g) and were implanted with mini-osmopumps (1004; ALZET) to infuse vehicle (0.154 mol/L NaCl/0.2% human serum albumin) or GLP-1(32-36)amide (50–70 nmol/kg body weight/day) over 12–19 weeks (19). During the infusion studies, body weights and food intake were monitored weekly and twice weekly, respectively. Fat and lean body mass were assessed on week 15 of the pentapeptide infusions using a whole-body dual X-ray scanner (Lunar Piximus; GE Medical Systems, Wauwatosa, WI).

Feed Efficiency
Feed efficiency (FE) (27) was evaluated during the infusions of vehicle or peptide as previously described (19).

Liver Histology, Triglyceride Content, and Plasma Triglyceride Levels
Tissue staining (hematoxylin-eosin) of livers and levels of triglycerides in liver extracts and plasmas (28) of mice at the end of the 15-week infusion and 32 weeks on high fat were determined as described previously (18).

Indirect Calorimetry and Locomotor Activity
Mice at 30 weeks on HFD and 12-week infusions with vehicle or GLP-1(32-36)amide were single caged for 5 days before placing them into individual metabolic chambers for 2 days for acclimatization, with free access to food and water. Oxygen consumption was determined by indirect calorimetry (TSE Systems). Oxygen consumption was measured at 5-min intervals for a total of 120 h. The results presented correspond to the last 6 h of the light cycle and 12 h of the dark cycle. Locomotor activity was determined by counting infrared light beam breaks (InfraMot Phenomaster/LabMaster cage system). Results are presented for the last 6 h of the light cycle and complete dark cycle and the average activity during both dark and light phases.

Fasting Plasma Glucose and Insulin and Glucose and Insulin Tolerance Tests
Plasma glucose and insulin levels were obtained in fasted (16 h) mice fed an HFD for 29 weeks and treated with

pentapeptide or vehicle for 12 weeks. Glucose tolerance tests were performed on mice at 24 weeks on HFD and 16-week infusions with vehicle or GLP-1(32-36)amide and were fasted overnight (16 h). Glucose (2 g/kg lean mass) was administrated by intraperitoneal injection. Blood samples were drawn from the tail vein at 0, 10, 30, 60, 120, and 140 min after glucose administration. Insulin tolerance tests were performed on mice at 38 weeks on HFD and 19-week infusions with either vehicle or GLP-1(32-36)amide. Mice were fasted for 4 h and given 0.75 units/kg lean mass insulin by intraperitoneal injection. Blood glucose was monitored at 0, 15, 30, 45, and 60 min after insulin injection. Blood draws were obtained by tail nick, and plasma glucose was measured using a glucometer OneTouch UltraMini glucose meter (LifeScan, Johnson & Johnson Company, Philadelphia, PA). Fasting insulin levels were determined using the rat/mouse ELISA kit (Crystal Chem, Downers, IL). Area under the curve (AUC) was determined by standard methods.

C2C12 Myotube Studies

C2C12 skeletal muscle cells were obtained from ATCC (Manassas, VA) and cultured in growing media (DMEM media: 25 mmol/L glucose, 10% FBS, and 1% penicillin and streptomycin) until differentiation when cells were cultured in differentiation media (DMEM: 25 mmol/L glucose, 2% horse serum, and 1% penicillin and streptomycin). Experiments were carried out at day 5 of differentiation. C2C12 myotubes were fasted for 6 h (no serum added) before incubation with GLP-1(32-36)amide (100 pmol/L) and/or 0.2 mmol/L palmitate:0.034 mmol/L BSA (5:1) for 16 h in fasting media.

Western Immunoblot Analysis

Cells lysates of C2C12 myotubes (15 μg), gastrocnemius muscle homogenates (15 μg), and BAT homogenates (10 μg) from in vivo mouse studies were resolved by SDS-PAGE, and proteins were analyzed by the Western immunoblot procedure as previously described (16) (see Fig. 5 legend).

Reactive Oxygen Species Determination

C2C12 myoblasts were seeded in 12-well fluorescence plates grown until confluence and differentiated to myotubes for 5 days. Reactive oxygen species (ROS) levels were determined in palmitate-treated myotubes as previously described (23) (see Fig. 6 legend).

Quantitative RT-PCR Assays of mRNA Levels

Mouse tissues were removed and immediately submerged in cold RNA*later* (QIAGEN, Valencia, CA) or frozen in liquid nitrogen. Total RNA was isolated and analyzed by quantitative PCR (qPCR) (CFX 384; Bio-Rad, Richmond, CA) as previously described (16). The primers used for qPCR are available upon request.

Statistics and Data Analyses

Data are presented as mean ± SEM. Statistical analyses were performed using Student *t* test. *P* values <0.05 were considered to be statistically significant.

RESULTS

Formation of GLP-1(32-36)amide

GLP-1(7-36)amide is rapidly cleaved in vivo (1–2 min) by Dpp4 to GLP-1(9-36)amide, a peptide devoid of significant insulinotropic activities (8) and is the major form of GLP-1 in the circulation. GLP-1(9-36)amide has insulin-like actions on heart, vasculature, and liver (10,16–19,24,28). Additional cleavages of GLP-1 occur by the endopeptidase NEP 24.11 in vitro, resulting in the formation of the nona- and pentapeptides GLP-1(28-36) amide and GLP-1(32-36)amide as major products, respectively (9) (Fig. 1*A*). To examine the formation of the pentapeptide by cleavage from GLP-1(9-36)amide in lean and obese mice, we administered GLP-1(9-36) amide by intraperitoneal injection and collected blood samples at 0, 5, 15, and 30 min for analyses of the levels of the peptides by semiquantitative LC-MS. GLP-1(9-36) amide appears in plasma within 5 min and was undetectable by 30 min, respectively, after the injection of GLP-1 (9-36)amide (Fig. 1*B*). At 5 min, the plasma concentrations of GLP-1(9-36)amide, GLP-1(28-36)amide, and GLP-1(32-36)amide in lean mice were 3.3 μmol/L, 4 μmol/L (data not shown), and 80 nmol/L, respectively (Fig. 1*B*). The plasma levels of the nona- and pentapeptides are 5- to 10-fold lower in the obese compared with the lean mice.
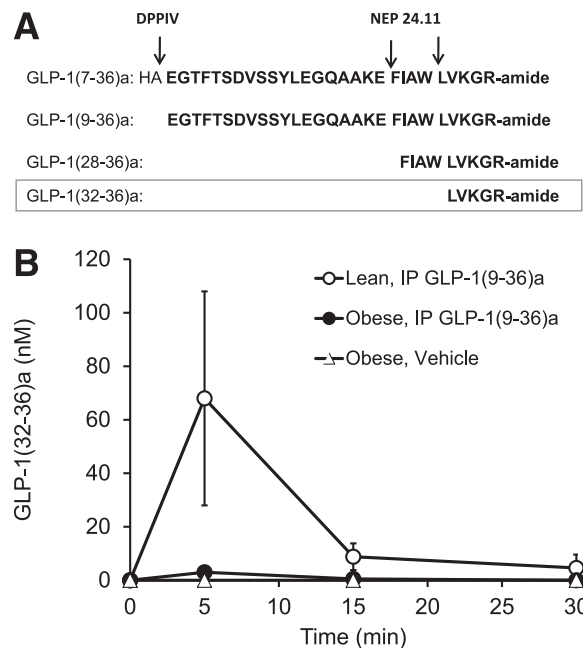

Figure 1—GLP-1(32-36)amide pentapeptide derived from GLP-1(9-36)amide. *A*: Formation of the C-terminal peptides GLP-1(9-36)amide, GLP-1(28-36)amide, and GLP-1(32-36)amide. *B*: Intraperitoneal (IP) administration of GLP-1(9-36)amide (500 μg) to mice results in the formation and appearance of GLP-1(32-36)amide in the plasma. Data obtained by a semiquantitative LC-MS assay (see RESEARCH DESIGN AND METHODS).

GLP-1(32-36)amide Prevents the Development of Diet-Induced Obesity and Hepatic Steatosis in High Fat–Fed Mice

At 6–10 weeks of age, mice were placed on an HFD for 17–18 weeks before beginning the continuous infusions of vehicle or GLP-1(32-36)amide for 12–16 weeks. The infusion of GLP-1(32-36)amide for 12 weeks attenuated the development of DIO (Fig. 2A). Mice receiving GLP-1(32-36)amide for 10 weeks gained less weight compared with vehicle control, at which time the peptide-treated mice began to lose weight (Fig. 2B). The average weekly change in body weight gain of mice infused with the pentapeptide was 50% less than that of mice receiving control vehicle over the 10-week infusion period (Fig. 2C). Caloric intakes in peptide- and vehicle-treated mice were similar (Fig. 2D). The FE indicated that 80% less of the caloric intake went into body weight in mice treated with the pentapeptide compared with vehicle (vehicle control, 0.016 ± 0.0018; pentapeptide treated, 0.003 ± 0.00075; $P = 0.06$).

Measurement of body fat and lean mass by DEXA between vehicle and GLP-1(32-36)amide mice treated for 16 weeks showed a 40% reduction in fat mass in the GLP-1(32-36)amide–infused mice compared with vehicle and no significant changes in lean mass (Fig. 2E and F). GLP-1(32-36)amide decreases liver fat accumulation when compared with vehicle, as shown in the hematoxylin-eosin staining liver tissue sections (Fig. 2G). The triglyceride contents in livers of mice receiving GLP-1(32-36)amide decreased by 60% when compared with vehicle and were similar to that of mice fed a regular chow diet (21.13 ± 5.6 mg/mL in livers of mice infused with GLP-1(32-36)amide compared with 21.6 ± 7 mg/mL protein in mice fed regular chow) (Fig. 2H). Moreover, the pentapeptide reduced both plasma glycerol levels (0.12 ± 0.025 mg/mL compared with 0.25 ± 0.04 mg/mL vehicle control; $P < 0.02$) and triglyceride levels (0.33 ± 0.06 mg/mL compared with 0.65 ± 0.06 mg/mL vehicle control; $P < 8E-04$) (Table 1).
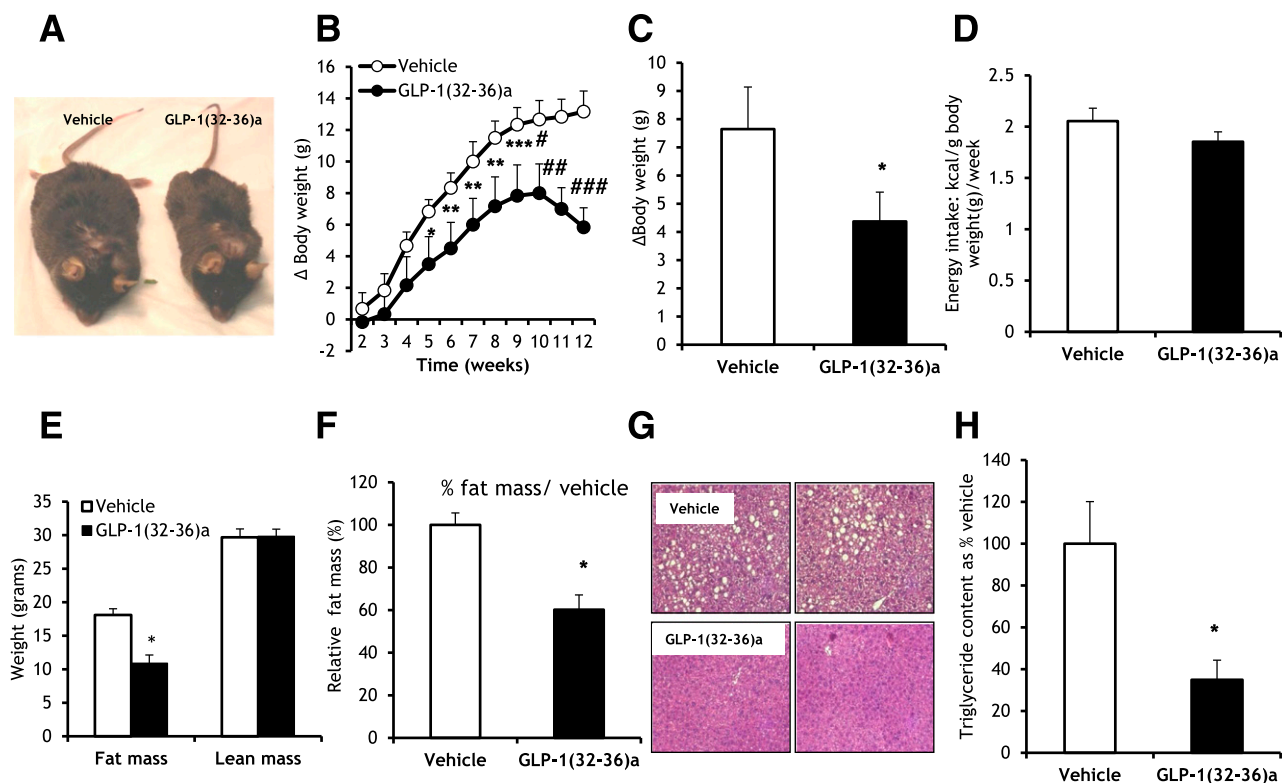

Figure 2—Continuous infusions of GLP-1(32-36)amide prevent the development of diet-induced obesity and attenuate the development of hepatic steatosis in mice fed an HFD. A: Photographs of representative mice infused with GLP-1(32-36)amide for 13 weeks. B: Curtailment of weekly body weight gain in mice fed an HFD in response to 12-week infusions of GLP-1(32-36)amide (n = 6 per group). Week 4, *P < 0.05; weeks 5–8, **P < 0.04; week 9, ***P < 0.03; week 10, #P < 0.01; week 11, ##P < 0.004; week 12, ###P < 1E-04, peptide vs. vehicle. C: Weekly incremental mean changes in body weights of data shown in B. *P < 0.04, peptide vs. vehicle (n = 6 per group). D: Energy intake during a 10-week period of vehicle and peptide infusions (n = 6 per group). E: Body composition of mice after 16-week infusions of vehicle and GLP-1(32-36)amide (n = 6 per group). *P < 0.008, peptide vs. vehicle. F: Fat mass expressed as percent of vehicle control from E. *P < 1.3E-03, peptide vs. vehicle. G: Representative sections of livers from mice treated with peptide or vehicle for 16 weeks. Sections are stained with hematoxylin and eosin. H: Triglyceride content of samples of livers in mice infused with GLP-1(32-36)amide for 15 weeks (n = 6 per group). Values are represented as percent vehicle control. *P < 0.005, peptide vs. vehicle. Liver triglyceride levels in HFD-fed mice receiving peptide infusions decrease to levels similar to those seen in mice fed a regular chow diet (21.5 ± 7.04).

diabetes.diabetesjournals.org

Table 1—Fasting plasma glucose, insulin, glycerol, and triglyceride in vehicle- and GLP-1(32-36)amide–treated DIO mice

	Vehicle	GLP-1 (32-36)amide
Plasma glucose (mmol/L)	8.89 ± 0.4	5.3 ± 0.4*
Plasma insulin (pmol/L)	296 ± 55.8	237.3 ± 50.8
Plasma glycerol (mg/mL)	0.25 ± 0.04	0.128 ± 0.025#
Plasma triglyceride (mg/mL)	0.65 ± 0.06	0.33 ± 0.02##

Continuous infusions of GLP-1(32-36)amide improve fasting plasma levels of glycerol and triglycerides and reduce fasting plasma levels of glucose and insulin. Plasma glycerol and triglyceride levels after 16-week infusions of peptide in mice fed an HFD for 24 weeks were decreased to levels of mice fed a low-fat normal chow diet (0.12 ± 0.02 and 0.58 ± 0.06, respectively) ($n = 6$ per group). Plasma glucose and insulin at 12-week infusions with GLP-1(32-36)amide and 2 weeks on HFD. #$P < 0.02$, peptide vs. vehicle. ##$P < 0.008$, peptide vs. vehicle. *$P < 1.3E-04$, peptide vs. vehicle.

GLP-1(32-36)amide Attenuates the Development of Fasting Hyperglycemia and Hyperinsulinemia and Improves Insulin Sensitivity in HFD Mice

Before beginning the treatment of DIO mice, the fasting glucose and insulin levels were similar among the two pretreatment groups of mice: vehicle mice (glucose, 4.8 ± 1.08 mmol/L; insulin, 209.2 ± 89.17 pmol/L) and peptide-treated mice (glucose, 4.3 ± 0.2 mmol/L; insulin, 116.7 ± 38 pmol/L). The infusions of GLP-1(32-36)amide for 12 weeks attenuated the progression of fasting hyperglycemia and hyperinsulinemia (Table 1).

To further determine the actions of GLP-1(32-36)amide on glucose homeostasis in DIO mice, intraperitoneal glucose and insulin tolerance tests were performed in mice receiving continuous infusions of the pentapeptide for 10 weeks. Mice fed an HFD for 24 weeks exhibited impaired glucose tolerance after the glucose challenge. The infusion of GLP-1(32-36)amide for 16 weeks resulted in an improvement in the glycemic excursion over the 140 min of the glucose tolerance test (Fig. 3A, left panel). Fasting plasma glucose and insulin levels at the beginning of the glucose tolerance challenge were reduced in GLP-1(32-36)amide–infused mice (glucose: 169.16 ± 7.5 mg/dL compared with 221.5 ± 8.6 mg/dL vehicle control [$P < 4.3E-04$], and insulin: 409.7 ± 65.2 pg/mL compared with 654.8 ± 129 pg/mL vehicle control). Mice receiving pentapeptide showed a lower AUC, indicating improved glycemic control (Fig. 3, upper right panel). Plasma insulin concentrations 10 min after glucose administration were higher in mice receiving GLP-1(32-36)amide (Fig. 3, lower right panel), a finding consistent with an increase in the insulin-to-glucose ratio in GLP-1(32-36)amide–infused mice (pentapeptide: 4.7 ± 1.78 compared with vehicle 1.5 ± 0.52; $P < 0.048$). Likewise, mice fed an HFD for 38 weeks and receiving GLP-1(32-36)amide for 19 weeks showed a more pronounced glucose-lowering response compared with that of vehicle-treated mice when challenged with an insulin tolerance test. These results suggest that mice infused with the pentapeptide are more insulin responsive when compared with the glucose response of vehicle-treated mice (Fig. 3B, right panel). The AUC glucose following insulin administration was lower in mice receiving GLP-1(32-36)amide than in vehicle-treated mice (Fig. 3B, left panel). Thus, GLP-1(32-36)amide administration protects the obese mice from the development of insulin resistance.

GLP-1(32-36)amide Increases Basal Metabolic Rate

To determine whether the attenuation of weight gain by GLP-1(32-36)amide was associated with changes in energy homeostasis, indirect calorimetry was performed in mice fed an HFD for 30 weeks and at the end of 12 weeks of treatment with GLP-1(32-36)amide. GLP-1(32-36)amide increased both total body and lean body resting oxygen consumption during the light and dark cycles (Fig. 4A and B, left panels). Total body oxygen consumption rates increased by 22 and 33% over the light and dark phases, respectively (Fig. 4A, right panel). No differences were observed between control and pentapeptide-treated mice in either energy intake (data not shown) or physical activity (Fig. 4C). Thus, these findings indicate that the regulatory effects of GLP-1(32-36)amide on energy homeostasis are associated with an increase in basal energy expenditure.

GLP-1(32-36)amide Increases the Expression of Uncoupling Proteins in BAT and Increases Fatty Acid Oxidation in Skeletal Muscle

Because of the finding of an increase in basal energy expenditure in the pentapeptide-treated mice, we examined BAT, a known thermogenic tissue (29,30), for effects of GLP-1(32-36)amide on the expression of uncoupling proteins. The protein expression of both UCP-1 and UCP-3 in BAT was significantly increased in mice infused with GLP-1(32-36)amide for 15 weeks and on an HFD for 32 weeks when compared with obese vehicle control mice (Fig. 5A and B). Likewise, mRNA expression for both UCP-1 and UCP-3 was increased by ~1.5–2-fold in mice receiving pentapeptide (Fig. 5C). The expression of the transcriptional coactivator PGC-1α, known to modulate the expression of UCP-1, oxidative metabolism, and thermogenesis in BAT (31), was increased in BAT of mice receiving the pentapeptide. Likewise, the expression of PPARα, known to have important actions in the modulation of fatty acid oxidation (32), was increased (Fig. 5C). Cytochrome C expression was also increased, although the increase did not reach statistical significance (Fig. 5C). Because skeletal muscle accounts for 20% of overall energy metabolism (33), we explored the role of skeletal muscle on energy homeostasis in obese mice treated with the pentapeptide. The ratio of phosphorylated to total ACC (pACC/ACC) was increased in gastrocnemius skeletal muscle of mice receiving GLP-1(32-36)amide for 16 weeks and on HFD for 24 weeks
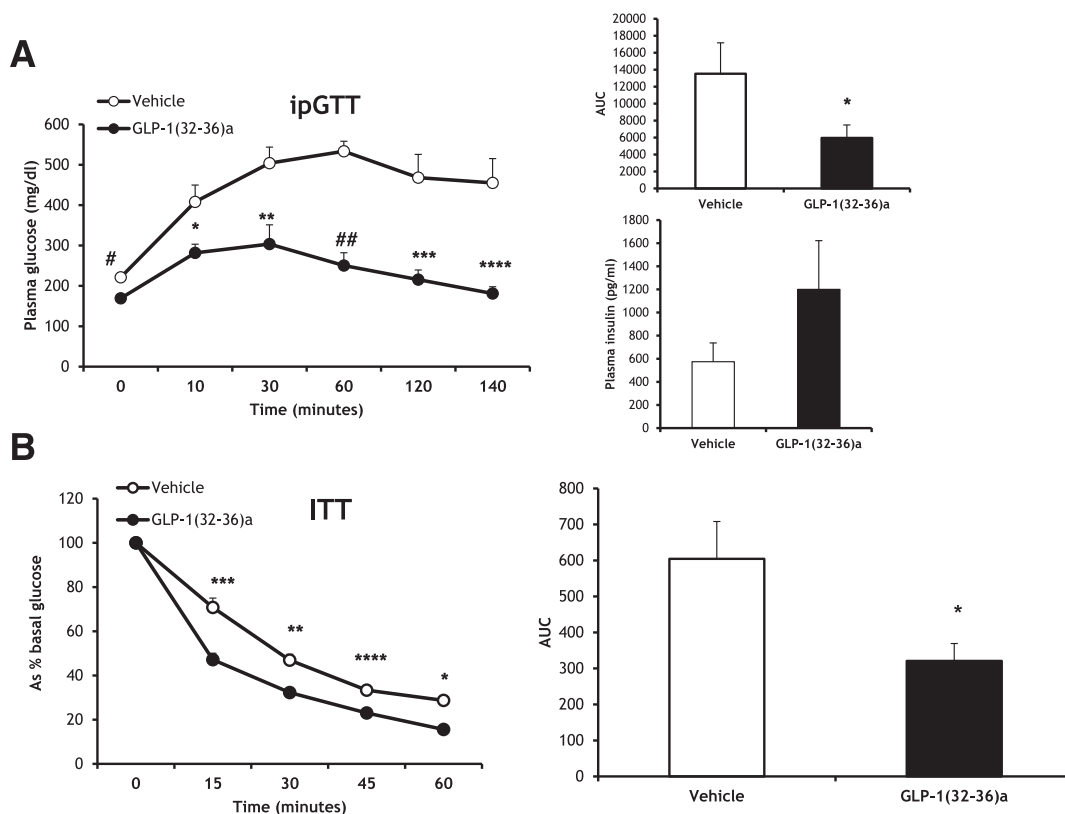
Figure 3—GLP-1(32-36)amide administration improves insulin sensitivity in DIO mice. *A*: Plasma glucose levels during an intraperitoneal glucose tolerance test (ipGTT) in mice fed an HFD for 24 weeks and 16 weeks of continuous infusions of vehicle or GLP-1(32-36)amide (*n* = 5–6 per group). #*P* < 2.8E-04; **P* < 0.0058; **P < 0.0028; ##*P* < 1.9E-05; ***P < 0.0018; ****P < 0.0014, peptide vs. vehicle. *Right upper panel*: Quantification of AUC for the total glycemic excursions (*n* = 5–6 per group). **P* < 0.046. *Right lower panel*: Plasma insulin concentrations obtained 10 min after glucose administration (*n* = 5–6 per group). *B*: Plasma glucose levels during an insulin tolerance test (ITT) in mice fed an HFD for 38 weeks and 19 weeks of continuous infusions of vehicle or GLP-1(32-36)amide (*n* = 4 per group). ***P < 1.2E-03; **P < 2.05E-03; ****P < 0.09E-03; **P* < 1.3E-03, peptide vs. vehicle. *Right panel*: Quantification of AUC for the total glycemic excursions (*n* = 4 per group). **P* < 0.02.

when compared with vehicle-treated mice (Fig. 5*D* and *E*). No changes were observed in skeletal muscle for UCP-3 protein (Fig. 5*D*), although UCP-3 mRNA was increased (Fig. 5*F*). Muscles of GLP-1(32-36)amide–treated mice showed either no change or a moderate increase in the transcription of genes associated with oxidative metabolism and/or mitochondrial biogenesis, such as PGC-1α, PPARα/γ, COX4i1, and COX7a1 (Fig. 5*F*). The expression of SCD-1 however was substantially decreased, suggesting a decrease in muscle adiposity, possibly due to an increase in fatty acid metabolism (Fig. 5*F*). Increased fatty acid oxidation in skeletal muscle might provide the fuel required to fulfill the energetic demands imposed by the increased energy expenditure in mice treated with the pentapeptide.

Similar findings of increased muscle oxidative phosphorylation were observed in C2C12 myotubes. The incubation of myotubes with GLP-1(32-36)amide (100 pmol/L) for 16 h increased both the ratio between phosphorylation of AMPK and the total expression of AMPK (pAMPK/AMPK) and the phosphorylation (inhibitory) of its downstream target ACC without differences in the expression of total ACC (Fig. 6*A*–*C*). Likewise, GLP-1(32-36)amide restored the

decreased phosphorylation of both AMPK and ACC phosphorylation in C2C12 myotubes in which oxidative metabolism had been impaired by pretreatment of the myotubes with palmitate for 16 h (Fig. 6*C* and *D*). In addition, GLP-1 (32-36)amide reduces intracellular levels of ROS induced in C2C12 myotubes by their treatment with palmitate (Fig. 6*E*).

DISCUSSION

Herein we describe the identification and the partial characterization of the actions of a pentapeptide, GLP-1 (32-36)amide (LVKGRamide), derived from the C terminus of the glucoregulatory hormone GLP-1. The pentapeptide appears to arise in the circulation via the cleavage of GLP-1 by an endopeptidase such as neprilysin (NEP 24.11) (9) or a related endopeptidase. Mass spectrometry detected the appearance of the pentapeptide in plasma after the intraperitoneal injection of GLP-1(9-36)amide in mice. The pentapeptide was postulated to exist in vivo based on the evidence that neprilysin generates the pentapeptide from GLP-1 (9), and a candoxatril-sensitive endopeptidase decreases levels of infused GLP-1 in the circulation of pigs (34).
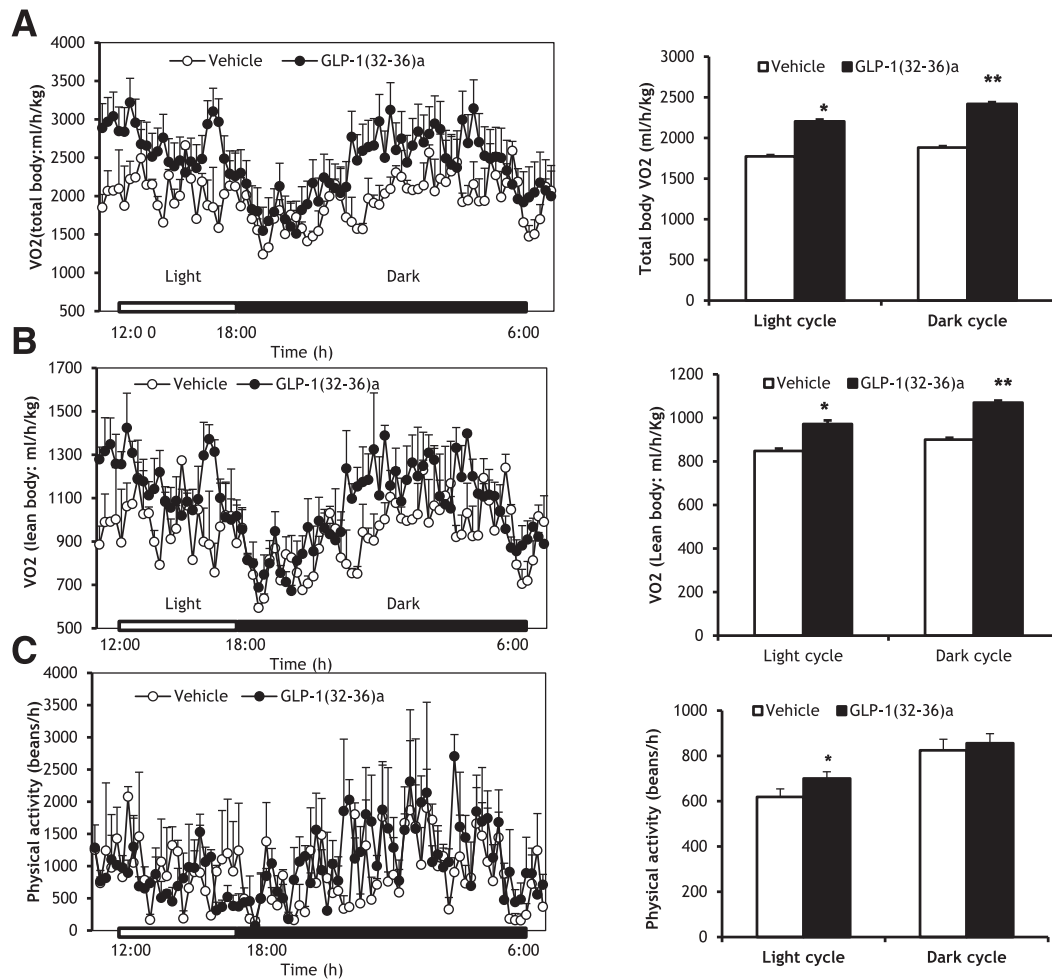
Figure 4—Increased energy expenditure in mice infused with GLP-1(32-36)amide and no changes in physical activity during the dark cycle. *A*: Whole-body oxygen consumption (VO2) in mice fed a very high-fat diet for 30 weeks and 12-week infusions of peptide (*n* = 2–3 per group). *Left panel*: Oxygen consumption was measured during the light and dark cycles. *Right panel*: Total oxygen consumption over the light and dark phases. *P < 5.9E−43; **P < 4E−66, peptide vs. vehicle control. *B*: Lean oxygen consumption (*n* = 2–3 per group). *Left panel*: Oxygen consumption was measured during light and dark cycles. *Right panel*: Total oxygen consumption over light and dark phases. *P < 1E−20; **P < 1E−35, peptide vs. vehicle. *C*: Assessment of physical activity. *Left panel*: Physical activity was measured during the light and dark cycles (*n* = 2–3 per group). *Right panel*: Total physical activity over the light and dark cycles. *P < 0.04, peptide vs. vehicle. The results correspond to the last 6 h of the light cycle and 12 h of the dark cycle (*A* and *B*, *left panel*) and the average values throughout the light and dark phases (*A* and *B*, *right panel*).

The pentapeptide is biologically active when infused into DIO mice and when added to cultured C2C12 myotubes. Pentapeptide infusions in DIO mice increase basal energy expenditure without effect on energy intake and inhibit weight gain and the development of insulin resistance and hepatic steatosis. Several observations indicate that increased energy expenditure is a major action of the pentapeptide. Pentapeptide-treated mice showed a 20–30% increase in oxygen consumption without significant changes in physical activity or food intake. Food intake was no different among vehicle control and treated groups. The FE showed that ~80% less of the caloric intake went into body weight in mice infused with the pentapeptide compared with vehicle control mice, indicating the existence of a substantial dissipation of the intake of caloric energy in pentapeptide-treated mice. Furthermore the pentapeptide increases the

expression of the uncoupling proteins UCP-1 and UCP-3 in BAT and decreases the activity of ACC in skeletal muscle of mice, indicative of increased fatty acid oxidation (35,36). The physiological mechanisms of GLP-1(32-36) amide on the inhibition of weight gain differ from those of GLP-1 receptor agonists. Receptor agonists inhibit energy intake with little or no effects on energy expenditure (37–40). Notably, basal energy expenditure is increased in mice lacking the GLP-1 receptor (41), suggesting a lowering of energy expenditure in response to receptor activation.

Although the precise mechanisms by which GLP-1(32-36)amide promotes energy expenditure remain unknown, one mechanism might be the uncoupling of mitochondrial respiration. Uncoupling dissipates energy in the form of heat (thermogenesis) and reduces mitochondrial energy overload and membrane charge and the formation of ROS
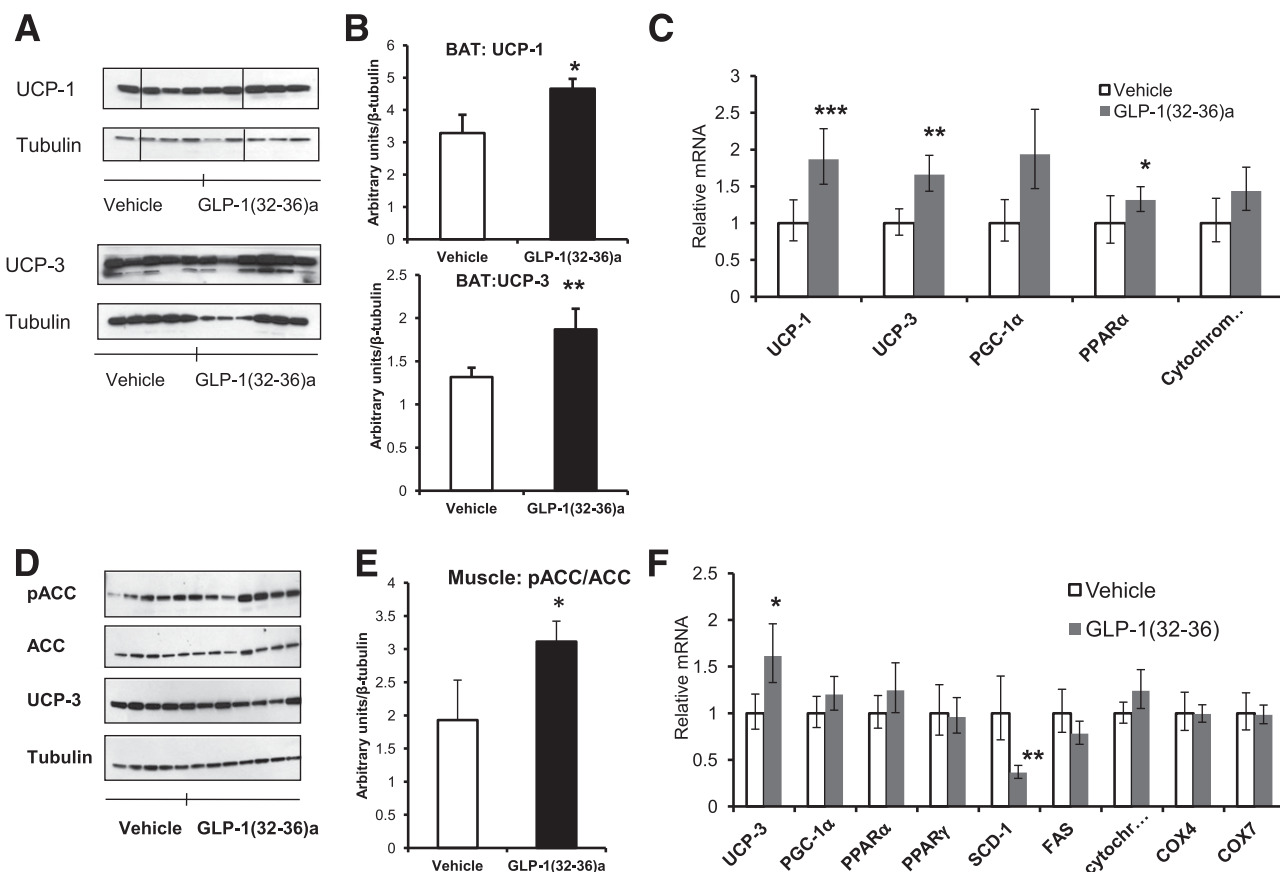
Figure 5—GLP-1(32-36)amide induces changes in the expression and/or phosphorylation of genes associated with thermogenesis and oxidative metabolism in BAT and skeletal muscle. *A*: UCP-1 and UCP-3 protein expression are increased in BAT of mice receiving GLP-1 (32-36)amide for 15 weeks and fed an HFD for 32 weeks as shown in Western blot analysis (n = 4–6 per group). *B*: Quantification of the Western blot images (*A*) of UCP-1 (*upper panel*) and UCP-3 (*lower panel*) (n = 4–6 per group). *$P < 0.028$; **$P < 0.03$, peptide vs. vehicle. *C*: qPCR showed enhanced expression of genes involved in thermogenesis and oxidative phosphorylation in BAT of mice infused with GLP-1 (32-36)amide for 15 weeks (n = 6 per group). *$P < 0.04$; **$P < 0.02$; ***$P < 0.01$, peptide vs. vehicle. *D*: Phosphorylation of ACC at Ser-79 compared with total expression of ACC is enhanced in skeletal muscle of mice infused with GLP-1(32-36)amide for 16 weeks and 24 weeks on an HFD as shown in Western blot analysis (n = 5–7 per group). No differences in UCP-3 protein levels were observed in skeletal muscle of mice receiving peptide compared with vehicle. *E*: Western blot image quantification (*C*) ratio between pACC and total ACC (pACC/ACC). *$P < 0.04$, peptide vs. vehicle. *F*: qPCR analysis of oxidative metabolism genes in gastrocnemius skeletal muscle of mice infused with GLP-1(32-36)amide for 15 weeks (n = 6 per group). *$P < 0.05$; **$P < 0.02$. Western immunoblots were assayed with anti-pACC (Ser-79) from Millipore (Billerica, MA), pAMPKα (Thr-172) and AMPKα from Cell Signaling Technology (Danvers, MA), anti-pACC (Ser-79) from Millipore (Billerica, MA), actin from Sigma-Aldrich, UCP-1 and UCP-3 from Abcam (Cambridge, MA), and tubulin (Santa Cruz Biotechnology) followed by secondary antibodies conjugated to horseradish peroxidase (Amersham Biosciences or Santa Cruz Biotechnology, Inc., Santa Cruz, CA). Protein bands were visualized by enhanced chemiluminescence and quantified by laser densitometry in the linear range. Results from cell culture and in vivo studies were normalized by actin and tubulin, respectively. Vertical lines were inserted to mark sites where the source autoradiographs were spliced to remove lanes of the intervening samples. Two lanes were removed in *A* because of gel loading artifacts. Four lanes were removed from the right of *D* because they contained samples unrelated to the subject matter of this report. All sample lanes were run on the same gel at the same time and all immunoblot analyses were conducted from the same samples.

(oxidative stress) (42). The findings of increased UCP-1 and UCP-3 expression in BAT and UCP-3 expression in skeletal muscle of mice treated with GLP-1(32-36)amide are consistent with an uncoupling of respiration. We suggest that the activation UCPs in BAT, and the resulting increased energy dissipation, contributes to the metabolic phenotype observed in the pentapeptide-treated mice. The transplantation of BAT tissue into either normal or DIO mice improves glucose tolerance, increases insulin sensitivity, and lowers body weight and fat mass (43).

A notable finding was the normalization of the hepatic triglyceride content in obese mice infused with the pentapeptide to levels found in lean mice fed a normal chow diet. This finding suggests that the peptide prevented, or possibly reversed, the development of hepatic steatosis. Although we did not measure triglyceride levels in the livers of the obese mice prior to starting the infusions of the pentapeptide, it is likely that the mice had fatty livers after 17 weeks on the HFD, the time that the infusions began. Male C57BL/6 mice characteristically develop simple hepatic steatosis and elevated levels of liver triglycerides by at least 12 weeks on the HFD (60 kcal fat) used in our studies (18).

In studies of cultured C2C12 skeletal myotubes, the pentapeptide activates the energy sensor AMPK, inhibits
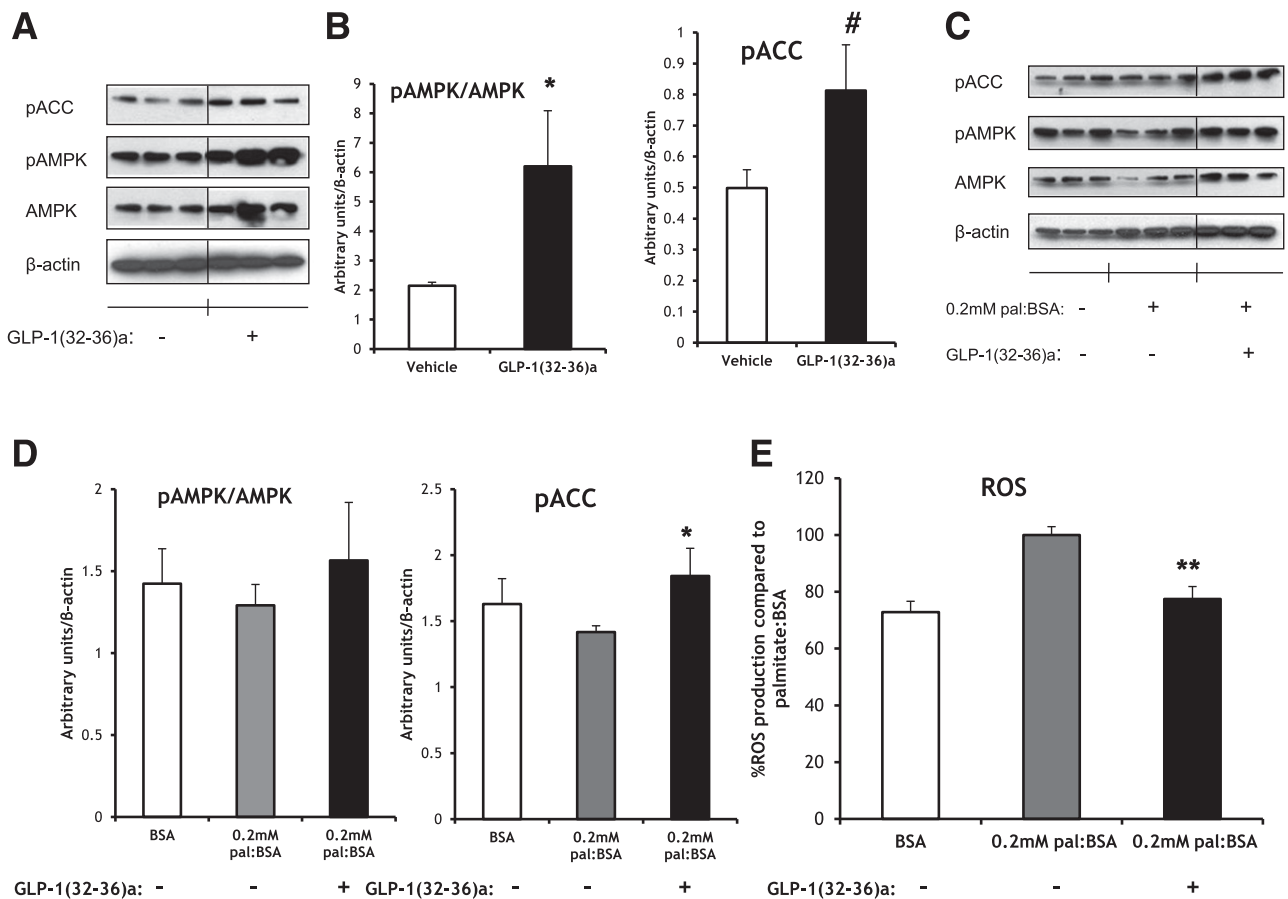
Figure 6—GLP-1(32-36)amide activates AMPK signaling, protects against palmitate-induced oxidative stress by restoring AMPK signaling, and reduces ROS levels in C2C12 myotubes. *A*: The incubation of C2C12 myotubes with GLP-1(32-36)amide (100 pmol/L) for 16 h increases the phosphorylation of AMPK at Thr-172 and its downstream target ACC at Ser-79 as shown in Western blot analysis. *B*: Quantification of the Western blot images of pACC (*right panel*) and the ratio between pAMPK and total AMPK (pAMPK/AMPK) (*left panel*). Data are the means ± SE. *$P < 0.05$; #$P < 3E-03$, peptide vs. vehicle. *C*: GLP-1(32-36)amide (100 pmol/L) restores the phosphorylation of ACC at Ser-79 reduced in palmitate (pal)-induced oxidative stress as shown in Western blot analysis. *D*: Quantification of the Western blot images of pACC (*right panel*) and the ratio of pAMPK to AMPK (*left panel*). Data are the means ± SE. *$P < 0.05$, peptide vs. vehicle. *E*: Levels of ROS of C2C12 myotubes exposed to palmitate:BSA (0.2 mmol/L:0.034 mmol/L) for 16 h in the absence or presence of GLP-1(32-36)amide (100 pmol/L). Data are expressed as percent production compared with palmitate:BSA and are the means ± SE. **$P < 7.6E-04$, peptide vs. vehicle. For ROS determination at day 5 of differentiation, cells were cultured in serum-free media for 6 h before the incubation with 0.2 mmol/L:0.034 mmol/L palmitate:BSA for 16 h in the presence or absence of GLP-1(32-36)amide (100 pmol/L) in fasting media. The following day, cells were rinsed twice in PBS and loaded with 5 μmol/L MitoSOX reagent (Invitrogen) in Hanks' balanced salt solution (HBSS)/Ca/Mg for 10 min at 37°C. Cells were then washed in HBSS/Ca/Mg for 10 min, and the same media was added during readings at 485/595 nm. Vertical lines were inserted to mark sites where the source autoradiographs were spliced to remove lanes of the intervening samples. Six and three lanes were removed from *A* and *C*, respectively, that contained concentrations of the pentapeptide apart from the focus of the study. All sample lanes were run on the same gel at the same time and all immunoblot analyses were conducted from the same samples.

ACC, and prevents an increase in levels of ROS in response to palmitate treatment. AMPK phosphorylates and inhibits ACC. ACC regulates the anabolism and catabolism of fatty acids via the formation of malonyl-CoA, both a substrate for the synthesis of fatty acids and an inhibitor of fatty acid oxidation. Inhibition of ACC reduces malonyl-CoA levels and relieves inhibition of carnitine palmitoyl transferase-1, required for the transport and oxidation of fatty acids in mitochondria. AMPK-mediated inhibition of ACC activity by the pentapeptide and enhanced fatty acid oxidation might account for the reduction in body fat mass observed in response to the pentapeptide.

The pentapeptide increased the transcriptional expression of UCP-3 in C2C12 myotubes and the skeletal muscle. Although the role of UCP-3 in skeletal muscle is controversial (44), it is believed that UCP-3 serves as a fatty acid transporter (29,30). The transport of fatty acids from the mitochondrial matrix to the outside of the inner membrane captures protons that are then carried retrograde back through the membrane to the matrix, thereby causing a proton leakage and energy dissipation (30,43).

We speculate that the de novo lipogenesis pathway might be modulated by GLP-1(32-36)amide. The findings of increased basal energy expenditure, activation of AMPK,

and increased fatty acid oxidation in pentapeptide-treated obese mice, coupled with an enhanced glucose disposal in hyperglycemic dogs in response (45), raises the possibility that GLP-1(32-36)amide might act via AMPK-responsive pathways similar to those activated by leptin that induce de novo lipogenesis in skeletal muscle (35). De novo lipogenesis would explain the findings of the effects of GLP-1 (32-36)amide on BAT and skeletal muscle as de novo lipogenesis, mediated by AMPK, links glucose uptake and fatty acid synthesis and oxidation with futile substrate cycling and facultative thermogenesis (31).

In summary, the findings described here suggest that GLP-1(32-36)amide might be an effective treatment for obesity and its related metabolic disorders in humans. In mice, the pentapeptide appears to modulate mitochondrial energy metabolism by increasing energy expenditure and fat metabolism, resulting in a reduction in rates of weight gain, body fat mass, oxidative stress, and insulin resistance. The pentapeptide is a product of the GLP-1 hormone naturally produced in the body. No adverse effects were observed in mice receiving continuous infusion of the pentapeptide for up to 16 weeks, suggesting that the pentapeptide might have a favorable safety profile, as well as efficacy in curtailing weight gain and possibly even promoting weight loss in humans. Whether or not the pentapeptide is active in humans, as well as in mice and dogs, awaits the results of clinical trials.

Duality of Interest. No potential conflicts of interest relevant to this article were reported.
Author Contributions. E.T. conceived of and performed the experiments, evaluated data, and prepared the figures and the manuscript. V.S. and K.M. participated in the experimental work and in the analysis of the data. A.K. synthesized, purified, and characterized the pentapeptide. P.E. and W.W.B. conducted and planned the mass spectroscopy experiments. J.F.H. conceived of experiments, evaluated data, and contributed to the manuscript. J.F.H. is the guarantor of this work and, as such, had full access to all the data in the study and takes responsibility for the integrity of the data and the accuracy of the data analysis.
Prior Presentation. Parts of this study were presented in abstract form at the 72nd Scientific Sessions of the American Diabetes Association, Philadelphia, PA, 8–12 June 2012; the 73rd Scientific Sessions of the American Diabetes Association, Chicago, IL, 21–25 June 2013; and the 74th Scientific Sessions of the American Diabetes Association, San Francisco, CA, 13–17 June 2014.

References

1. Tateya S, Kim F, Tamori Y. Recent advances in obesity-induced inflammation and insulin resistance. Front Endocrinol (Lausanne) 2013;4:93
2. Hoehn KL, Salmon AB, Hohnen-Behrens C, et al. Insulin resistance is a cellular antioxidant defense mechanism. Proc Natl Acad Sci U S A 2009;106:17787–17792
3. Grattagliano I, Palmieri VO, Portincasa P, Moschetta A, Palasciano G. Oxidative stress-induced risk factors associated with the metabolic syndrome: a unifying hypothesis. J Nutr Biochem 2008;19:491–504
4. Haas JT, Biddinger SB. Dissecting the role of insulin resistance in the metabolic syndrome. Curr Opin Lipidol 2009;20:206–210
5. Lovshin JA, Drucker DJ. Incretin-based therapies for type 2 diabetes mellitus. Nat Rev Endocrinol 2009;5:262–269
6. Kieffer TJ, Habener JF. The glucagon-like peptides. Endocr Rev 1999;20:876–913
7. Plamboeck A, Holst JJ, Carr RD, Deacon CF. Neutral endopeptidase 24.11 and dipeptidyl peptidase IV are both involved in regulating the metabolic stability of glucagon-like peptide-1 in vivo. Adv Exp Med Biol 2003;524:303–312
8. Deacon CF. Circulation and degradation of GIP and GLP-1. Horm Metab Res 2004;36:761–765
9. Hupe-Sodmann K, McGregor GP, Bridenbaugh R, et al. Characterisation of the processing by human neutral endopeptidase 24.11 of GLP-1(7-36) amide and comparison of the substrate specificity of the enzyme for other glucagon-like peptides. Regul Pept 1995;58:149–156
10. Tomas E, Habener JF. Insulin-like actions of glucagon-like peptide-1: a dual receptor hypothesis. Trends Endocrinol Metab 2010;21:59–67
11. Nikolaidis LA, Elahi D, Shen YT, Shannon RP. Active metabolite of GLP-1 mediates myocardial glucose uptake and improves left ventricular performance in conscious dogs with dilated cardiomyopathy. Am J Physiol Heart Circ Physiol 2005;289:H2401–H2408
12. Ban K, Noyan-Ashraf MH, Hoefer J, Bolz SS, Drucker DJ, Husain M. Cardioprotective and vasodilatory actions of glucagon-like peptide 1 receptor are mediated through both glucagon-like peptide 1 receptor-dependent and -independent pathways. Circulation 2008;117:2340–2350
13. Sonne DP, Engstrøm T, Treiman M. Protective effects of GLP-1 analogues exendin-4 and GLP-1(9-36) amide against ischemia-reperfusion injury in rat heart. Regul Pept 2008;146:243–249
14. Ban K, Kim KH, Cho CK, et al. Glucagon-like peptide (GLP)-1(9-36)amide-mediated cytoprotection is blocked by exendin(9-39) yet does not require the known GLP-1 receptor. Endocrinology 2010;151:1520–1531
15. Green BD, Hand KV, Dougan JE, McDonnell BM, Cassidy RS, Grieve DJ. GLP-1 and related peptides cause concentration-dependent relaxation of rat aorta through a pathway involving KATP and cAMP. Arch Biochem Biophys 2008;478:136–142
16. Tomas E, Stanojevic V, Habener JF. GLP-1 (9-36) amide metabolite suppression of glucose production in isolated mouse hepatocytes. Horm Metab Res 2010;42:657–662
17. Elahi D, Egan JM, Shannon RP, et al. GLP-1 (9-36) amide, cleavage product of GLP-1 (7-36) amide, is a glucoregulatory peptide. Obesity (Silver Spring) 2008;16:1501–1509
18. Tomas E, Stanojevic V, Wood JA, Habener JF. Glucagon-like peptide-1(9-36)amide metabolite inhibits weight gain and attenuates diabetes and hepatic steatosis in diet-induced obese mice. Diabetes Obes Metab 2011;13:26–33
19. Tomas E, Wood JA, Stanojevic V, Habener JF. GLP-1-derived nonapeptide GLP-1(28-36)amide inhibits weight gain and attenuates diabetes and hepatic steatosis in diet-induced obese mice. Regul Pept 2011;169:43–48
20. Shao W, Wang Z, Ip W, et al. GLP-1(28-36) improves β-cell mass and glucose disposal in streptozotocin-induced diabetic mice and activates cAMP/PKA/β-catenin signaling in β-cells in vitro. Am J Physiol Endocrinol Metab 2013;304:E1263–E1272
21. Liu Z, Stanojevic V, Brindamour LJ, Habener JF. GLP1-derived nonapeptide GLP1(28-36)amide protects pancreatic β-cells from glucolipotoxicity. J Endocrinol 2012;213:143–154
22. Ip W, Shao W, Chiang YT, Jin T. GLP-1-derived nonapeptide GLP-1(28-36) amide represses hepatic gluconeogenic gene expression and improves pyruvate tolerance in high-fat diet-fed mice. Am J Physiol Endocrinol Metab 2013;305:E1348–E1358
23. Tomas E, Stanojevic V, Habener JF. GLP-1-derived nonapeptide GLP-1 (28-36)amide targets to mitochondria and suppresses glucose production and oxidative stress in isolated mouse hepatocytes. Regul Pept 2011;167:177–184
24. Abu-Hamdah R, Rabiee A, Meneilly GS, Shannon RP, Andersen DK, Elahi D. Clinical review: the extrapancreatic effects of glucagon-like peptide-1 and related peptides. J Clin Endocrinol Metab 2009;94:1843–1852

25. Merrell K, Southwick K, Graves SW, Esplin MS, Lewis NE, Thulin CD. Analysis of low-abundance, low-molecular-weight serum proteins using mass spectrometry. J Biomol Tech 2004;15:238–248

26. Kuzyk MA, Smith D, Yang J, et al. Multiple reaction monitoring-based, multiplexed, absolute quantitation of 45 proteins in human plasma. Mol Cell Proteomics 2009;8:1860–1877

27. Parekh PI, Petro AE, Tiller JM, Feinglos MN, Surwit RS. Reversal of diet-induced obesity and diabetes in C57BL/6J mice. Metabolism 1998;47:1089–1096

28. Bligh EG, Dyer WJ. A rapid method of total lipid extraction and purification. Can J Biochem Physiol 1959;37:911–917

29. Krauss S, Zhang CY, Lowell BB. The mitochondrial uncoupling-protein homologues. Nat Rev Mol Cell Biol 2005;6:248–261

30. Echtay KS. Mitochondrial uncoupling proteins—what is their physiological role? Free Radic Biol Med 2007;43:1351–1371

31. Lin J, Handschin C, Spiegelman BM. Metabolic control through the PGC-1 family of transcription coactivators. Cell Metab 2005;1:361–370

32. Lefebvre P, Chinetti G, Fruchart JC, Staels B. Sorting out the roles of PPAR alpha in energy metabolism and vascular homeostasis. J Clin Invest 2006;116: 571–580

33. Rolfe DF, Brown GC. Cellular energy utilization and molecular origin of standard metabolic rate in mammals. Physiol Rev 1997;77:731–758

34. Plamboeck A, Holst JJ, Carr RD, Deacon CF. Neutral endopeptidase 24.11 and dipeptidyl peptidase IV are both mediators of the degradation of glucagon-like peptide 1 in the anaesthetised pig. Diabetologia 2005;48:1882–1890

35. Dulloo AG, Gubler M, Montani JP, Seydoux J, Solinas G. Substrate cycling between de novo lipogenesis and lipid oxidation: a thermogenic mechanism against skeletal muscle lipotoxicity and glucolipotoxicity. Int J Obes Relat Metab Disord 2004;28(Suppl. 4):S29–S37

36. Xue B, Kahn BB. AMPK integrates nutrient and hormonal signals to regulate food intake and energy balance through effects in the hypothalamus and peripheral tissues. J Physiol 2006;574:73–83

37. Shalev A, Holst JJ, Keller U. Effects of glucagon-like peptide 1 (7-36 amide) on whole-body protein metabolism in healthy man. Eur J Clin Invest 1997;27:10–16

38. Gu W, Lloyd DJ, Chinookswong N, et al. Pharmacological targeting of glucagon and glucagon-like peptide 1 receptors has different effects on energy state and glucose homeostasis in diet-induced obese mice. J Pharmacol Exp Ther 2011;338:70–81

39. Bradley DP, Kulstad R, Racine N, Shenker Y, Meredith M, Schoeller DA. Alterations in energy balance following exenatide administration. Appl Physiol Nutr Metab 2012;37:893–899

40. Tan TM, Field BC, McCullough KA, et al. Coadministration of glucagon-like peptide-1 during glucagon infusion in humans results in increased energy expenditure and amelioration of hyperglycemia. Diabetes 2013;62:1131–1138

41. Hansotia T, Maida A, Flock G, et al. Extrapancreatic incretin receptors modulate glucose homeostasis, body weight, and energy expenditure. J Clin Invest 2007;117:143–152

42. Brookes PS. Mitochondrial H(+) leak and ROS generation: an odd couple. Free Radic Biol Med 2005;38:12–23

43. Stanford KI, Middelbeek RJ, Townsend KL, et al. Brown adipose tissue regulates glucose homeostasis and insulin sensitivity. J Clin Invest 2013;123: 215–223

44. Bézaire V, Seifert EL, Harper ME. Uncoupling protein-3: clues in an ongoing mitochondrial mystery. FASEB J 2007;21:312–324

45. Elahi D, Angeli FS, Vakilipour A, et al. GLP-1(32-36)amide, a novel pentapeptide cleavage product of GLP-1, modulates whole body glucose metabolism in dogs. Peptides 2014;59:20–24